Research paper

Targeting nanoparticles to M cells with non-peptidic ligands for oral vaccination

Virginie Fievez [a,b,1], Laurence Plapied [a,1], Anne des Rieux [a], Vincent Pourcelle [c], Hélène Freichels [d], Valentine Wascotte [a], Marie-Lyse Vanderhaeghen [a], Christine Jerôme [d], Alain Vanderplasschen [e], Jacqueline Marchand-Brynaert [c], Yves-Jacques Schneider [b], Véronique Préat [a,*]

[a] Université catholique de Louvain, Unité de Pharmacie Galénique, Brussels, Belgium
[b] Université catholique de Louvain, Laboratoire de Biochimie cellulaire, toxicologique et nutritionnelle, Institut des Sciences de la Vie, Louvain-la-Neuve, Belgium
[c] Université catholique de Louvain, Unité de Chimie Organique et Médicinale, Louvain-la-Neuve, Belgium
[d] Université de Liège, Centre d'Etudes et de la Recherche sur les Macromolécules, Liège, Belgium
[e] Université de Liège, Immunologie-Vaccinologie, Département des Maladies infectieuses et parasitaires, Faculté de Médecine vétérinaire, Liège, Belgium

ARTICLE INFO

ABSTRACT

The presence of RGD on nanoparticles allows the targeting of β1 integrins at the apical surface of human M cells and the enhancement of an immune response after oral immunization. To check the hypothesis that non-peptidic ligands targeting intestinal M cells or APCs would be more efficient for oral immunization than RGD, novel non-peptidic and peptidic analogs (RGD peptidomimitic (RGDp), LDV derivative (LDVd) and LDV peptidomimetic (LDVp)) as well as mannose were grafted on the PEG chain of PCL–PEG and incorporated in PLGA-based nanoparticles. RGD and RGDp significantly increased the transport of nanoparticles across an in vitro model of human M cells as compared to enterocytes. RGD, LDVp, LDVd and mannose enhanced nanoparticle uptake by macrophages in vitro. The intraduodenal immunization with RGDp-, LDVd- or mannose-labeled nanoparticles elicited a higher production of IgG antibodies than the intramuscular injection of free ovalbumin or intraduodenal administration of either non-targeted or RGD-nanoparticles. Targeted formulations were also able to induce a cellular immune response. In conclusion, the in vitro transport of nanoparticles, uptake by macrophages and the immune response were positively influenced by the presence of ligands at the surface of nanoparticles. These targeted-nanoparticles could thus represent a promising delivery system for oral immunization.

© 2009 Elsevier B.V. All rights reserved.

1. Introduction

Most human vaccines currently available are licensed for non-mucosal administration via subcutaneous or intramuscular routes [1]. However, most pathogens gain access to their hosts via the mucosal surfaces. It would thus be beneficial to develop mucosal vaccines that would avoid pain and the risks of infection associated with injections and could make large-population immunization more feasible [2]. Moreover, the administration of an antigen at one mucosal site can lead to the generation of an immune response, not only locally but also at distant mucosal sites, a phenomenon referred to as the common mucosal immune system [3].

Several vaccines have been developed for oral administration. These include bacterial vaccines against cholera and typhoid fever and viral vaccines against polio and, recently, rotavirus infections.

All these vaccines are based on live attenuated or inactivated organisms, which elicit both humoral and cellular immunity. However, their intrinsic instability makes them difficult to deliver and raises safety issues as a reversion to an invasive state may occur [4,5]. Killed or inactivated whole organism vaccines generate a weaker immune response and require multiple doses [6]. Modern vaccinology focuses on a new generation of vaccines composed of purified sub-units that are, in many cases, protein or peptide antigens. However, these antigens are poorly absorbed when administered orally, mainly due to their low mucosal permeability and their lack of stability in the gastro-intestinal environment. Their immunogenicity is considerably lower than that of traditional vaccines [7]. To overcome these problems, their association with adjuvants that act as delivery systems, such as polymeric particles and/or modulators of the immune response such as cholera toxin B, have been widely investigated [4,8]. The use of polymeric nanoparticles for the delivery of complex antigens, a combination of antigens, and genetic vaccines makes them one of the most promising strategies for oral vaccination [2,8].

Polymeric carriers protect antigens against degradation and inactivation in the harsh gastro-intestinal environment [7] and

have the ability to enhance their transmucosal transport [8]. Besides all of these advantages, the lack of efficacy of these particulate systems to induce an immune response by the oral route has been frequently reported, possibly a consequence of poor particle uptake, and up to now none of them has reached the market. To enhance the efficacy of orally delivered antigen-loaded particles, methods increasing their uptake and their transcytosis by M cells seem particularly attractive [8]. M cells are specialized epithelial cells, located in the follicle-associated epithelium (FAE) of Peyer's patches [9]. They have high transcytotic capabilities and are able to transport a broad range of materials, such as bacteria, viruses, antigens and particles from the intestinal lumen to the underlying lymphoid tissues [10,11]. The morphology of M cells promotes the interaction of these materials with their apical membrane. Moreover, their basolateral membrane is deeply invaginated, forming a pocket hosting immune cells (antigen presenting cells (APC) and lymphocytes) [9]. As M cells are present at a very low density in the gut, specific targeting of M cells could enhance particle uptake by M cells [8]. Even if there is a lack of specific markers of human M cells, $\beta 1$ integrins have been shown to be overexpressed at the apical pole of human M cells [12,13]. We have demonstrated that grafting RGD that targets this integrin on the PEG chain of PLGA-based nanoparticles significantly increased their *in vitro* transport by M-like cells. Nevertheless, targeted-nanoparticles containing ovalbumin only slightly increased the IgG immune response after oral immunization [12]. We hypothesised that this was due to a partial degradation of the RGD peptide during its trafficking through the gastro-intestinal tract.

The aim of this study was to encapsulate a model antigen in a polymer-based formulation in order to (i) target the apical surface of human M cells using non-peptidic ligands to avoid ligand degradation in the gastro-intestinal tract and (ii) achieve a cellular and humoral immunization after oral delivery. Various ligands were grafted on the PEG chain of PCL–PEG and incorporated in PLGA-based nanoparticles. Four ligands targeting $\beta 1$ integrin were grafted: RGD as the peptidic reference, RGD peptidomimetic (RGDp), LDV derivative (LDVd) and LDV peptidomimetic (LDVp). This selection of ligands relies upon literature and in-house data. RGD molecules (oligopeptides, cyclic peptides and peptidomimetics) have been widely used in biomaterials science for stimulating cellular adhesion on surfaces via integrin receptors because such molecules mimic the cell attachment sites of various extracellular matrix proteins [14]. Although the RGD peptides target a lot of integrin sub-types, the tyrosine-based RGD peptidomimetics have been recently shown to interact selectively with the beta 3 and beta 1 sub-types [15–17]. On the other hand, LDV peptides are selective ligands of beta 1 integrin and their affinity could be improved by chemical modification with a diarylurea motif [18]. Similarly, LDV peptidomimetics featuring a diarylurea motif behaved as selective beta 1 ligands [19,20]. This integrin-targeting strategy was compared to the targeting of APC where mannose was selected as the ligand of macrophages and dendritic cells [21–23]. The influence of these different ligands on nanoparticle transcytosis through the intestinal epithelium or FAE and on their ability to induce an immune response after oral vaccination was evaluated *in vitro* and *in vivo*, respectively.

2. Materials and methods

2.1. Materials

2.1.1. Chemicals and solvents

Reagents and solvents were of analytical grade and purchased from Acros (Beerse, Belgium) and Sigma–Aldrich–Fluka (Bornem, Belgium). Monomethoxypoly(ethylene glycol), triethylaluminum

(1.9 M in toluene), N,N'-dicyclohexylcarbodiimide, dibutyltin dimethoxide, fluorescein, 4-(dimethylamino)pyridine, monomethoxypoly(ethylene glycol) (PEG), sodium cholate, tin(II) octanoate were purchased from Sigma–Aldrich–Fluka. ϵ-Caprolactone (99%) was purchased from Sigma–Aldrich–Fluka and was dried over $CaH2$ and distilled before use. D,L-lactide and glycolide were obtained from PURAC (Gorinchem, NL) and were purified and dried before use. Methylene dichloride and acetonitrile were obtained from Acros. The radiolabeled L-[4,5-3H] lysine monohydrochloride in aqueous solution was purchased form Amersham Biosciences (Little Chalf-ont, UK) with a specific activity of 89.0 Ci/mmol.

2.1.2. Cell culture

Human colon carcinoma Caco-2 cell line (clone 1) was obtained from Dr. Maria Rescigno, University of Milano-Bicocca (Milano, IT) and used from passage $x + 12$ to $x + 30$. The Human Burkitt's lymphoma Raji B line was purchased from American Type Culture Collection (Manassas, VA) and used from passage 102 to 110. The J774 murine macrophage cell line was obtained from ECACC (Salisbury, UK). Dulbecco modified Eagle's minimal essential medium (DMEM, 25 mM glucose), RPMI 1640 medium, non-essential amino acids, L-glutamine and penicillin–streptomycin, Hank's balanced salt solution buffer (HBSS), phosphate buffer saline (PBS), trypsin (0.25%) with EDTA were purchased from Gibco™ Invitrogen Corporation (Carlsbad, CA). Heat-inactivated fetal calf serum was obtained from Hyclone (Perbio Sciences, Erembodegem, BE). Transwell® polycarbonate inserts (12 wells, pore diameter of 3 μm), cell culture plates 24 wells and 96 wells (flat bottom) and T-Flask for cell culture were purchased from Corning Costar (New York, NY). Anti-$\beta 1$ integrin antibody was obtained from USBiological (Massachusetts, US) and the Polyclonal rabbit anti-ovalbumin antibody from Abcam (ab1221, Cambridge, UK). Albumin from bovine serum for molecular biology, Albumin from chicken egg white (Grade V, $\geqslant 98\%$), TWEEN® 20 and Triton® X-100 were purchased from Sigma–Aldrich–Fluka. Cytotoxicity Detection Kit (LDH) was obtained from Roche Diagnostic GmbH (Mannheim, DE).

2.1.3. Immunizations and ELISA

Specific pathogen-free female Balb/C mice aged 6 weeks were purchased from JANVIER (Le Genest-Saint-Isle, FR). Ketamine (Ketalar) was obtained from Pfizer (BE), xylazine from Sigma–Aldrich–Fluka, Iodine solution (Iso-Betadine) from Meda (BE) and plates from Nunc-Immuno (Plate F96 MAXISORP, Thermo Fisher Scientific, Langenselbold, DE). Peroxidase-labeled rat anti-mouse immunoglobulin G was obtained from LO-IMEX (Brussels, BE), Ficoll–Hypaque from Beckman coulter (ANALIS SA, Suarlée, BE), Mouse IFN-γ and IL-4 DuoSet ELISA development kits from R&D Systems (Europe Ltd., Abingdon, UK).

2.2. Polymers synthesis and characterization

2.2.1. Polymer synthesis

PLGA was prepared as previously described [24], by copolymerization of lactide and glycolide promoted by the dibutyltin dimethoxide as the catalyst [12]. To obtain the fluorescent polymer, fluorescein with a carboxylic acid function was prepared according to the method described by Cao et al. [25] and then was coupled to the MeO-PLGA-OH using N,N'-dicyclohexylcarbodiimide as the coupling agent and 4-(dimethylamino)pyridine as the catalyst. PEG-b-PLGA was synthesized as previously described [26], by a conventional ring-opening polymerization of D,L-lactide and glycolide using PEG as the macroinitiator and stannous octanoate as the catalyst [27]. The PEG–PCL copolymer was also synthesized by ring-opening polymerization using triethylaluminum as the catalyst [28].

2.2.2. Polymer characterization

^{1}H NMR (400 MHz) spectra were recorded in CDCl$_3$ at 25 °C with a Brüker AM 400 apparatus (Labbay, Geldermalsen, NL). Size-exclusion chromatography (SEC) was carried out in THF at a flow rate of 1 mL/min at 45 °C using an SFD S5200 auto-sampler liquid chromatograph (Chemie.DE, Berlin, DE) equipped with a SFD refractometer index detector 2000 and columns PL gel 5 μm (columns porosity: 102, 103, 104 and 105 Å). Polystyrene standards were used for calibration. The polymers used for the preparation of nanoparticles and PCL–PEG used for grafting are described in Table 1.

2.3. Ligands

The ligands grafted on the polymers described in Fig. 1 were the following:

RGD: Gly-Arg-Gly-Asp-Ser (GRGDS) pentapeptide (97%) was purchased from NeoMPS (Polypeptide Laboratories Group, Strasbourg, FR).

RGDp: This Arg-Gly-Asp (RGD) peptidomimetic, based on the tyrosine template, was designed and synthesized according to protocols adapted from Biltresse et al. [15,16].

LDVd: This Leu-Asp-Val (LDV) tripeptide derivative, with a diaryl urea motif at N-terminus and a triethyleneglycol spacer-arm at C-terminus, was prepared by standard peptide synthesis in solution, according to protocols adapted from Lin et al. [19].

LDVp: A LDV peptidomimetic was synthesized as described by Momtaz et al. [20].

Man: Mannose derivative, namely 2-aminoethyl-α-D-mannopyroside (MannOH–NH$_2$), was synthesized as previously described [29].

2.4. Grafting of ligand on PCL–PEG by photografting

PCL–PEG (13,200–5000) was solubilized in methylene dichloride or acetonitrile with O-succinimidyl 4-(p-azidophenyl) butanoate as previously described [29] (0.6 mmol per gram of PCL–PEG). After solvent evaporation, the sample was irradiated at 254 nm in a quartz flask under an argon atmosphere for 20 min. After washing, the "activated" sample was immersed in a 1 mM solution of ligand in phosphate buffer (0.1 M)/acetonitrile (1:1, v/v) at pH 8 and shaken for 24 h at 20 °C. Then the sample was washed and dried under a vacuum at 40 °C to constant weight.

As previously described [29,30], the grafting rates were controlled with a tritiated probe (L-[4,5-^{3}H] lysine monohydrochloride). 2946 nmol of covalently fixed probes per gram of copolymer were attained. The absolute amount of MannOH–NH$_2$ contained in the products was determined by the phenol–sulphuric acid method and the amounts of 5425 ± 2 nmole of MannOH–NH$_2$ were covalently grafted per gram of copolymer.

Fig. 1. Ligands grafted on PCL–PEG.

2.5. Preparation and characterization of nanoparticles

Nanoparticles were prepared by the "water-in-oil-in-water" solvent evaporation method as reported by Garinot et al. [12]. Briefly, 50 μL of a 75 mg ovalbumin/mL PBS was emulsified with 1 mL of methylene dichloride containing 50 mg of polymers (70% PLGA/15% PLGA–PEG/15% PCL–PEG with or without the ligand) with an ultrasonic processor (70 W, 15 s). The second emulsion was performed with 2 mL of 1% (w/v) sodium cholate aqueous solution. The double emulsion was then poured into 100 mL of a 0.3% sodium cholate aqueous solution and stirred at 37 °C for 45 min. The nanoparticle suspension was then washed twice in PBS by centrifugation at 22,000g for 1 h.

Fluorescent nanoparticles were prepared by incorporating PLGA–FITC instead of PLGA in the formulations.

2.6. Characterization of ovalbumin-loaded nanoparticles

Nanoparticle size and zeta potential were determined in KCl 0.1 mM using the Zetasizer Nano Series Malvern [12] (Worcestershire, UK).

Nanoparticles were centrifuged and supernatants collected. The loading efficiency and the loading capacity were determined by quantifying the unbound ovalbumin in the supernatant with the

Table 1
Polymers characteristics.

Polymer	Mn (SEC)[a] (g/mol)	Mn (NMR)[b] (g/mol)	Mn[c] PEG	Mn[d] PCL	Glycolide (mol%)	Polydispersity index (PDI)[e]
PLGA	22,000	–	–	–	25	1.8
Fluorescent–PLGA	23,600	–	–	–	29	1.6
PEG–b–PLGA	29,300	4600–16,500 (L)/4700 (G)	–	–	26	1.7
PCL–b–PEG	18,200	–	5000	13,200	–	1.4

[a] Polystyrene calibration.

[b] Determined by NMR with the following formula: $(I_{4.7}/2)/(I_{52} + (I_{4.7}/2)) * 100$, where $I_{4.7}$ is the signal intensity of the glycolide unit at 4.7 ppm (CH$_2$OCdbnd;O) and is the signal intensity of the lactide unit at 5.2 ppm (CH(CH$_3$)OCdbnd;O).

[c] Calculated from ^{1}H NMR spectrum in CDCl$_3$ at 25 °C by comparing the intensity of the terminal methyl group (CH$_2$OCH$_3$, 3.2 ppm) with the methylene protons (OCH$_2$CH$_2$O, 3.6 ppm).

[d] Calculated from ^{1}H NMR spectrum in CDCl$_3$ at 25 °C by comparing the intensity of the methylene protons of PEG peak at 3.6 ppm, with the peak of the α-methylene protons of PCL at 4.05 ppm.

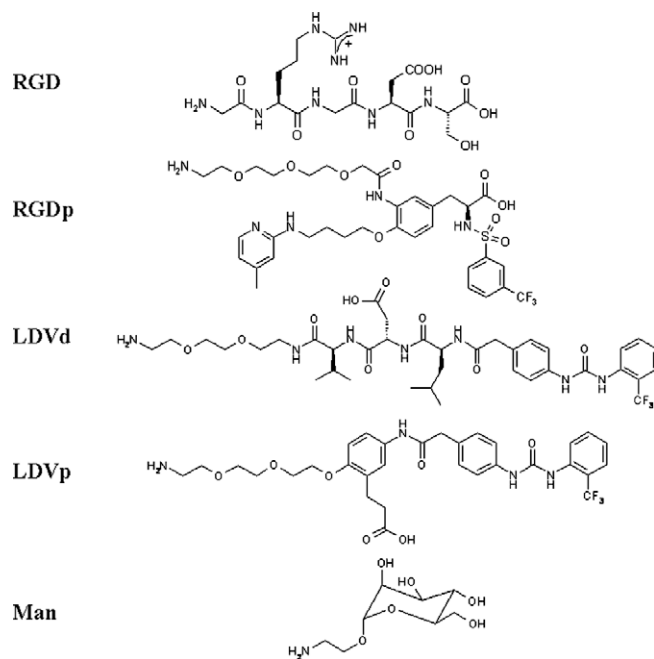[e] PDI = Mw/Mn, determined by SEC by polystyrene standard.

Micro BCA Protein assay Kit (Pierce PERBIO, Erembodegem, BE) [12]. Both loading efficacy (LE) and loading capacity (LC) were determined as follows:

$$LR\ (\%) = \frac{\text{Total amount of OVA} - \text{Free OVA}}{\text{Total amount of OVA}}$$

$$LC\ (\mu g/mg) = \frac{\text{Total amount of OVA} - \text{Free OVA}}{\text{Amount of polymer in nanoparticles}}$$

Nanoparticles were dissolved with 0.15 M NaOH containing 7.5% (w/v) SDS at 100 °C for 3 min [31]. SDS–polyacrylamide gel electrophoresis (SDS–PAGE) under reducing conditions was used to evaluate the integrity of the ovalbumin after its encapsulation in polymeric nanoparticles. Dissolved nanoparticles were filtered through 1 μm (Millipore low binding protein), concentrated on 30 KDa Amicon filters and loaded onto 11% (w/v) acrylamide gel. Proteins were visualized by silver staining and Western blot using a polyclonal rabbit anti-ovalbumin antibody at a 1/3000 dilution.

2.7. Nanoparticle transport across the in vitro M cells model

2.7.1. In vitro model of the human FAE
Caco-2 cells and Raji cells were grown as previously described [32,12]. The inverted in vitro model of the human FAE was obtained as described by des Rieux et al. [32]. Briefly, 3–5 days after Caco-2 cells seeding, the inserts were inverted. After 9–11 days, Raji cells were added in the basolateral compartments. The co-cultures were maintained for 5 days. Mono-cultures of Caco-2 cells were used as controls. Inserts were used in their original orientation for all the following in vitro experiments. Cell monolayer integrity, both in co- and mono-cultures, was controlled by transepithelial electrical resistance (TEER) measurement using an EndohmTM tissue resistance chamber (Endohm-12, World Precision Instruments, Sarasota, FL) connected to a Millicell®-RES (Millipore, Billerica, MA) ohmmeter.

2.7.2. Transport experiments
Transport experiments were run in HBSS at 37 °C. The nanoparticle concentration was adjusted by diluting the stock solution (checked by FACS analysis, FACScan, Becton Dickinson, Erembodegem, BE) [32,12] in HBSS to a final concentration of 2.7×10^{10} nanoparticles per milliliter. After equilibration in HBSS at 37 °C, the apical medium of the cell monolayers was replaced by a nanoparticle suspension (400 μL) and inserts were incubated at 37 °C over 90 min. For the inhibition study, cells were apically pre-incubated with an anti-β1 integrin antibody at 5 μg/mL in HBSS for 1 h at 37 °C, before adding nanoparticle suspensions at a final concentration of 2.7×10^{10} nanoparticles/mL. The inhibitor was present throughout the whole transport experiment (90 min at 37 °C). Basolateral solutions were then sampled and the number of transported nanoparticles was measured using a flow cytometer (FACScan) [32,12].

Results are expressed as apparent permeability coefficient (Papp) [33] (mean ± standard error of the mean (SEM)). The absence of cytotoxicity of the different formulations was assessed by measuring the TEER values after each experiment and lactate dehydrogenase (LDH) activity released from the cytosol of damaged cells into the apical medium.

The Papp is defined by the following formula:

$$Papp = dQ/dt A C_0$$

where dQ/dt is the number of nanoparticles (np) present in the basal compartment as a function of time (s); A, the area of Transwell (cm^2); and C_0, the initial concentration of nanoparticles in apical compartment (np/mL).

2.8. Uptake of nanoparticles by macrophages

Murine macrophages of the cell line J774 were employed to study the phagocytic uptake of PLGA-based nanoparticles. The J774 murine macrophage cell line was maintained as an adherent culture and was grown as a monolayer in a humidified incubator at 37 °C in 175 cm² flasks (Corning Costar) containing RPMI 1640 medium supplemented with 10% (v/v) FCS, 1% (v/v) penicillin–streptomycin, 1% (v/v) L-glutamine and 1% (v/v) non-essential amino acids. Cells were detached with a trypsin–EDTA solution and adjusted to the required concentration of viable cells. For nanoparticles uptake, macrophages were seeded in 24-well plate at 5.5×10^5 cells/cm² and left to adhere for 48 h at 37 °C in a humidified atmosphere of 5% (v/v) CO_2. Before the uptake experiment, cells were washed twice with free RPMI 1640 and left for 30 min. Fluorescent nanoparticles were diluted in HBSS at final concentration of 3×10^8 nanoparticles/ml. Cells were incubated with 500 μl of the nanoparticle solution for 60 min at 37 °C. After incubation, cells were washed twice with cold HBSS, twice with cold HBSS containing 0.1% (w/v) BSA and 0.2% Tween 20, and twice with cold HBSS to remove non-associated nanoparticles. After that these cells were incubated in a 0.1% (v/v) Triton® X-100 solution to release the nanoparticles that had been internalized by the macrophages. Nanoparticles were counted by FACS. Results are expressed as a percentage of the number of nanoparticles in the donor compartment.

2.9. Oral immunization with ovalbumin-loaded nanoparticles

The mice were kept in hanging wire cages and allowed to feed and drink ad libitum. Mice were fasted the day before their immunization. Protocols were approved by the ethical committee for animal care of the faculty of medicine of Université catholique de Louvain.

For the first oral vaccination study, five groups of eight mice were vaccinated by intragastric gavage with the following formulations containing ovalbumin: non-targeted PLGA nanoparticles, RGD-nanoparticles, LDVd-nanoparticles, LDVp-nanoparticles and man-nanoparticles or free ovalbumin. As positive and negative controls, two groups of eight mice were also immunized by intramuscular injection with ovalbumin and PBS, respectively.

For the second immunization study, six groups of eight mice were vaccinated by intraduodenal injection with the following formulations containing ovalbumin: non-targeted nanoparticles, RGD-nanoparticles, RGDp-nanoparticles, LDVd-nanoparticles, LDVp-nanoparticles and man-nanoparticles. As positive and negative controls, one group of eight mice was immunized by intramuscular injection with ovalbumin and two groups of eight mice were immunized by intraduodenal injection with free ovalbumin and empty PLGA nanoparticles. For the intraduodenal administration, the animals were anesthetized by intraperitoneal administration with ketamine (50 mg/kg) and xylazine (15 mg/kg). The abdomen was shaved and disinfected with iodine solution immediately before surgery. The abdomen was opened by a small central incision, and meticulous care was taken to prevent blood loss. Formulations and control solutions were injected into the mouse duodenum immediately distal to the stomach. The injections were performed by insertion of a 0.5-in., 27-gauge needle oblique to the intestinal lumen. The incision in the peritoneum was sutured using 5-0 Polyglactin 910 (Vicryl, J&J, BE) and the skin using 6-0 Monofilament Nylon (Monosof, US Surgical, USA). The surgical procedure lasted approximately 15 min per animal.

For all vaccination studies, mice were immunized on days 0 and 14 with 50 μg of ovalbumin free or loaded in particles in 100 μl each time. Blood samples were collected by retro-orbital puncture

on days 12, 28 and 42. Sera isolated by centrifugation were stored at −20 °C before analysis. Ovalbumin-specific IgG levels were evaluated by ELISA [12]. Sera dilutions were made in ovalbumin-coated plates and the detection of anti-ovalbumin antibodies was carried out using peroxidase-labeled rat anti-mouse immunoglobulin G (total IgG). Mice were sacrificed 6 weeks post-immunization and spleens were removed aseptically. Splenocytes were purified on Ficoll–Hypaque density gradient centrifugation and were cultivated in a humidified incubator at 37 °C in 96-well plates containing RPMI 1640 medium, supplemented with 10% (v/v) FCS, 1% (v/v) penicillin–streptomycin, 1% (v/v) L-glutamine and 1% (v/v) non-essential amino-acids. Splenocytes were stimulated with free ovalbumin (10 μg/well) in triplicates. After 48 h and 72 h, cell-free culture supernatants were harvested and analysed for IFN-γ and IL-4 production, respectively, by ELISA [12].

2.10. Statistics

Particle transport across the co- and mono-culture cell monolayers was compared using ANOVA parametric tests ($p < 0.05$) and immunization studies were analysed by Kruskal–Wallis non-parametric tests ($p < 0.05$).

3. Results

3.1. Physicochemical characterization of the nanoparticles

Formulations were characterized in terms of size, zeta potential, loading efficiency and loading capacity of ovalbumin (Table 2). All nanoparticles had a mean size around 200 nm with a small poly-dispersity index. The zeta potentials of all formulations were slightly negative when measured in 0.1 mM KCl.

The molecular weight and the integrity of encapsulated ovalbumin were checked by SDS–PAGE gel electrophoresis. Identical bands were observed for entrapped ovalbumin compared to native ovalbumin. Ovalbumin integrity was also detected by Western Blot (data not shown). Encapsulation of ovalbumin in nanoparticles did not seem to alter the integrity of the protein.

3.2. In vitro transport of targeted nanoparticles by enterocytes and FAE

To evaluate the ability of the different ligands to target the apical surface of M cells, the transport by mono-culture of Caco-2 cells (enterocytes) or co-cultures of Caco-2 cells and Raji cells (FAE) of nanoparticles displaying different targeting molecules was compared (Fig. 2A). Nanoparticles were incubated on the apical side of the mono- and co-cultures, at 37 °C, over a period of 90 min. The average TEER values for each group were approximately 300 and 170 Ω/cm² for mono- and co-cultures, respectively. The different nanoparticles did not influence the TEER during the transport experiment. For each formulation, the transport across co-cultures was significantly higher than that across mono-cultures ($p < 0.05$). As previously observed [12], the presence of PCL–PEG–GRGDS in the formulation significantly increased the transport of nanoparticles across the co-cultures when compared to non-targeted nanoparticles. RGDp had the same effect on the nanoparticle transport as RGD, increasing their transport by co-cultures three times, when compared to non-targeted nanoparticles. An inhibition of the transport of the RGD- and RGDp-nanoparticles by co-cultures was observed in the presence of the anti-integrin β1 antibody in the apical compartment ($p < 0.05$) (Fig. 2B). No significant difference between the uptakes of LDVd- and LDVp-nanoparticles was observed and the transport rates across mono- and co-cultures were comparable to non-targeted nanoparticle transport. Mannose-labeling of nanoparticles was able to increase their transport by both mono- and co-cultures, when compared with non-targeted nanoparticles.

3.3. Uptake of nanoparticles by macrophages

Their uptake by macrophages was also investigated in order to check whether the ligands grafted on the nanoparticles could affect

Table 2
Physicochemical properties of the ovalbumin-loaded nanoparticles containing PLGA (70%)/PLGA–PEG (15%)/PCL–PEG with or without grafted ligands (15%) ($n = 3$–5).

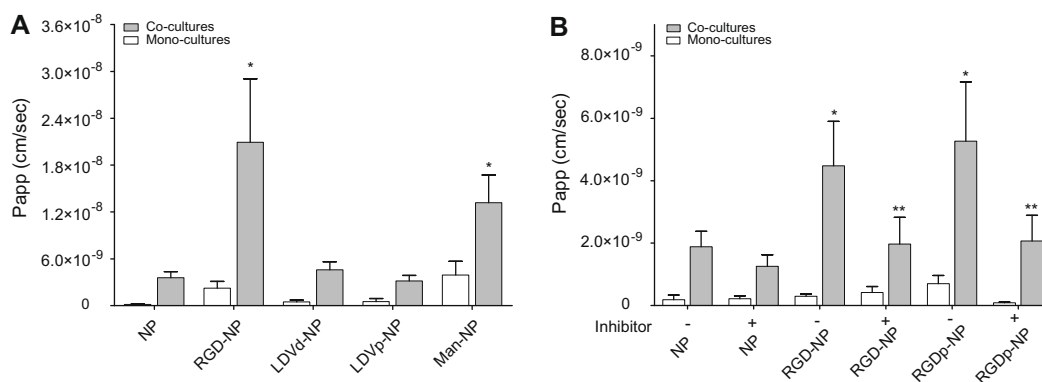|	Non-targeted	RGD	RGDp	LDVd	LDV p	Man
Size (nm)	220 ± 30	215 ± 29	230 ± 25	222 ± 24	221 ± 28	260 ± 24
Pdi	0.235	0.205	0.250	0.255	0.226	0.300
Zeta potential (mV)	−18 ± 5	−18 ± 6	−20 ± 6	−15 ± 5	−13 ± 5	−22 ± 6
Loading efficiency (%)	15.7 ± 0.5	19.7 ± 2.6	17.6 ± 3	16.2 ± 3	18.4 ± 2	18.2 ± 3
Loading capacity (μg OVA/mg polymer)	11.8 ± 0.4	14.8 ± 2	13.2 ± 2	12.2 ± 3	14.8 ± 1.5	13.7 ± 2

Fig. 2. Influence of ligand grafting on nanoparticle transport across mono- and co-cultures of Caco-2 cells. (A) Cell monolayers were incubated for 90 min at 37 °C with 2.7×10^{10} nanoparticles/ml of each formulation suspended in HBSS. (B) Cell monolayers were first apically pre-incubated with anti-β1 integrin (inhibitor+) or without (inhibitor−) at 5 μg/ml in HBSS for 1 h at 37 °C, before adding nanoparticle suspension at a final concentration of 2.7×10^{10} nanoparticles/ml. The number of transported nanoparticles was evaluated by flow cytometry and is expressed as apparent permeability coefficient (Papp) as a mean ± standard error of the mean (SEM). *$p < 0.05$: vs. NP, **$p < 0.05$: inhibitor vs. no inhibitor ($n = 24$).
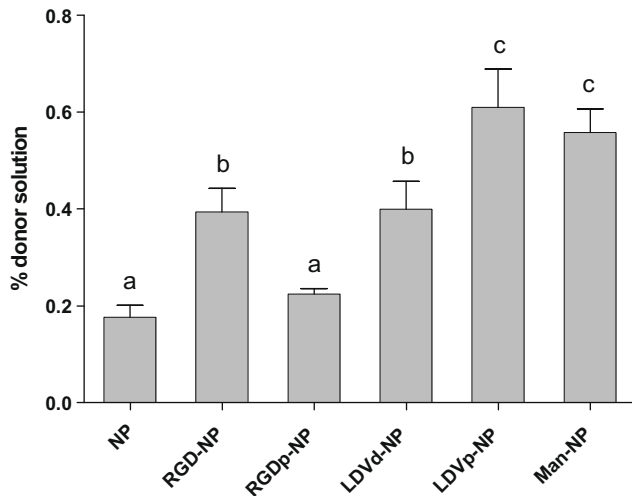
Fig. 3. Influence of ligand grafting on nanoparticle uptake by macrophages. Cell monolayers were incubated for 60 min at 37 °C with 500 µl of each formulation (3×10^8 nanoparticles/ml) suspended in HBSS. The relative affinity of the nanoparticles for the macrophages was evaluated by flow cytometry and is expressed as percentage of the donor solution as a mean ± standard error of the mean (SEM). Group b is significantly different from group a ($p < 0.05$) and group c is significantly different from group a ($p < 0.001$) ($n = 24$).

their uptake by APCs. Quantification of nanoparticles uptake by J774 cells revealed that the presence of the ligand at the nanoparticle surface also influenced the uptake of nanoparticles by macrophages (Fig. 3). After 60 min. of incubation at 37 °C, LDVp and mannose-nanoparticles were three times more internalized by macrophages than non-targeted nanoparticles, confirming previous results where the uptake of man-nanoparticles by macrophages was 50% higher than that of the uncoated nanoparticles [34]. RGD and LDVd labeling of nanoparticles doubled nanoparticle internalization by macrophages when compared to non-targeted nanoparticles, whereas RGDp labeling of nanoparticles did not influence the uptake of nanoparticles by these cells.

3.4. Oral immunizations studies

3.4.1. Intragastric administration of ovalbumin-loaded nanoparticles

Mice were immunized twice with 50 µg of ovalbumin by gavage in order to evaluate the potential of the different formulations as oral vaccine delivery systems. The IgG concentration was deter-mined by the measure of the optical density obtained after ELISA realized on sera sampled 6 weeks after priming. Results are expressed in function of the serum dilution factor (Fig. 4A). In addition, the optical densities at the 1/320 dilution of the serum of each mouse are displayed in Fig. 4B. The number of non-responding mice was relatively high, and differences were not statistically significant due to the high variability within the groups. However, LDVd-nanoparticles increased the number of responding mice (three mice out of eight), inducing an increase of mean total IgG seric concentration. As expected, free ovalbumin did not elicit an immune response and all mice responded to ovalbumin administered by IM injection.

3.4.2. Intraduodenal administration of ovalbumin-loaded nanoparticles

To avoid a possible degradation of the nanoparticle or of their associated ligands in the stomach and to concentrate the formulation at the site of absorption, intraduodenal injection of the same amount of ovalbumin (2×50 µg/mice) was used to perform a second immunization study (Fig. 5). All mice vaccinated with ovalbumin-loaded nanoparticles showed a strong and significant enhancement in the IgG production against ovalbumin when compared to the immune response obtained after intragastric administration. A low immune response was observed in the group vaccinated with free ovalbumin, while no response was elicited by empty PLGA nanoparticles. Mice immunized with non-targeted, RGD- and LDVp-nanoparticles produced a systemic immune response, identical to the immune response elicited by the IM route. RGDp-, LDVd- and man-nanoparticles elicited the higher IgG response, although only RGDp-nanoparticles allowed induction of an immune response significantly different from the group immunized with free ovalbumin. The isotype of ovalbumin-specific serum IgG at day 42 is shown in Fig. 6. Intraduodenal administration of ovalbumin-loaded nanoparticles elicited predominantly IgG1 and some IgG2a antibodies.

The cellular immune response was evaluated by measuring the IFN-γ production of splenocytes cultured in the presence of ovalbumin. A significant trend towards enhanced IFN-γ responses was observed in groups of mice immunized with ovalbumin loaded in nanoparticles compared with the response elicited by IM injection or by intraduodenal administration of free ovalbumin. Splenocytes from the groups immunized with LDVd- and man-nanoparticles produced a very low amount of IFN-γ, while the others targeted formulations produced a high level of IFN-γ (Fig. 7). The IL-4 production by splenocytes remained very low (<30 pg/ml, data not shown).
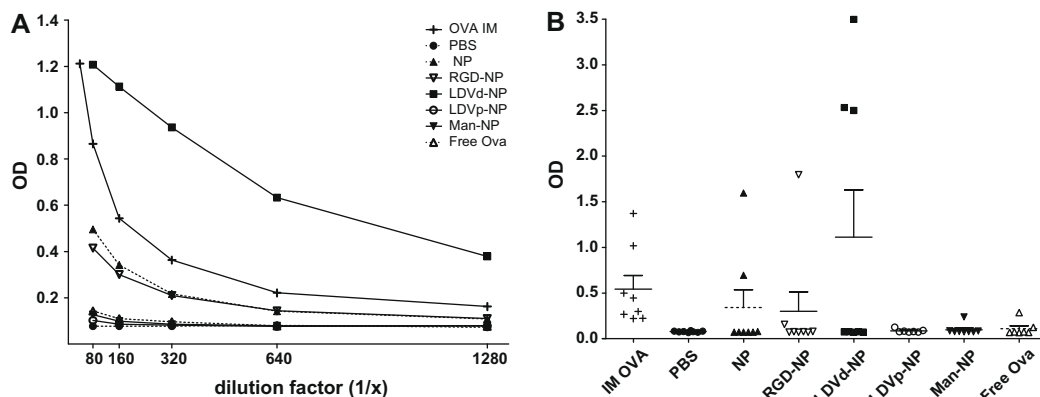

Fig. 4. Influence of the ligand grafting at the nanoparticle surface on IgG$_{tot}$ concentration in serum of mice immunized by gavage with 2×50 µg of ovalbumin free or encapsulated (blood sampling 6 weeks after priming). (A) Mean of absorbance obtained after ELISA for each group in function of the serum dilution factor. (B) Mice individual absorbance obtained after ELISA at the 1/320 dilution of the serum ($n = 8$).
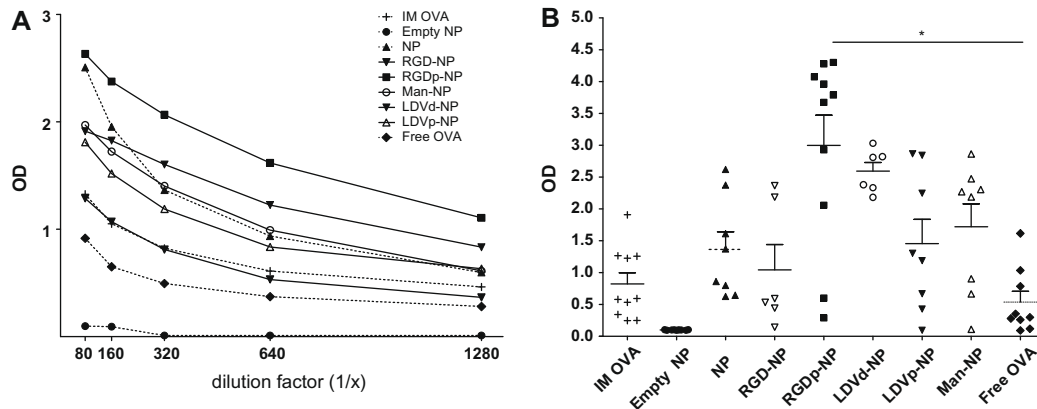
Fig. 5. Influence of the ligand grafting at the nanoparticle surface on IgG_{tot} concentration in serum of mice immunized by intraduodenal administration with 2×50 µg of ovalbumin free or encapsulated (blood sampling 6 weeks after priming). (A) Mean of absorbance obtained after ELISA for each group in function of the serum dilution factor. (B) Mice individual absorbance obtained after ELISA at the 1/320 dilution of the serum ($n = 6$–10). $^*p < 0.05$.
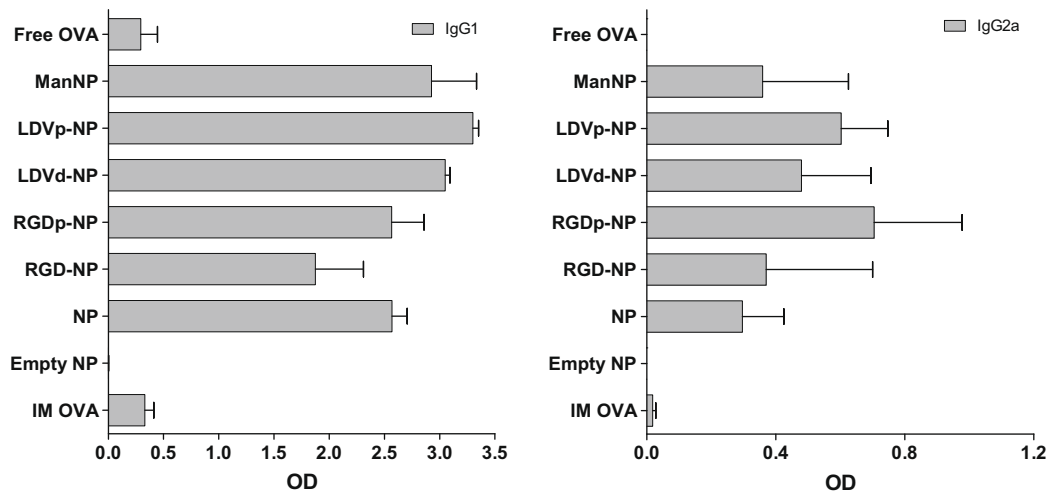

Fig. 6. Influence of the ligand grafting at the nanoparticle surface on IgG1 and IgG2a profile in serum of mice immunized by intraduodenal administration with 2×50 µg of ovalbumin free or encapsulated (blood sampling 6 weeks after priming). Results are presented as a mean ± standard error of the mean (SEM) of absorbance obtained after ELISA for each group at the 1/160 dilution of the serum ($n = 6$–10). Immune response elicited by mice vaccinated with the empty nanoparticles was considered as the blank and was subtracted from the other responses.
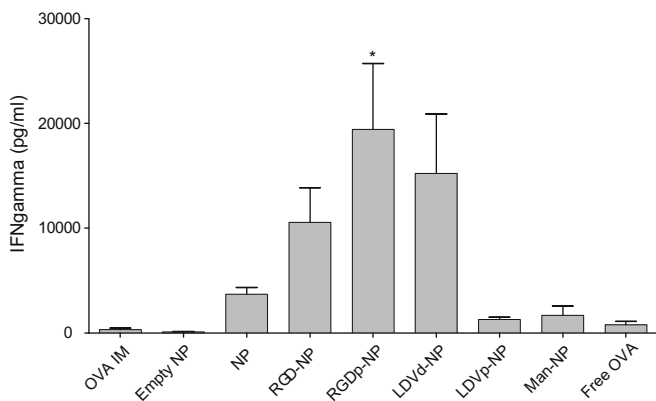

Fig. 7. Influence of the ligand grafting at the nanoparticle surface on IFN-γ production by splenocytes of mice immunized by intraduodenal administration with 2×50 µg of ovalbumin free or encapsulated (splenocytes culture 6 weeks after priming). Results are expressed in pg/ml as a mean ± standard error of the mean (SEM) ($n = 6$–10). $^*p < 0.05$.

4. Discussion

The aim of this study was to develop non-peptidic ligands targeting intestinal M cells or APCs for oral immunization. Hence, PCL–PEG labeled by photografting with different ligands was included in PLGA-based nanoparticles of 200 nm [12]. The presence of the ligands on the PEG chain and at the surface of the nanoparticles was demonstrated by XPS [30]. The efficiency of ligand photografting was also assessed (3000–5000 pmole per gram of polymer) [29]. Even though grafting of RGD on the nanoparticles has been shown to enhance their transport by M cells and elicit immune response after oral immunization [12], we hypothesised that using novel non-peptidic ligand would enhance the stability of the ligand in the gastro-intestinal tract and enhance the immune response after oral vaccination.

To investigate the influence of the targeting moiety on their transport through the intestinal epithelium, in vitro studies performed on a model of the human FAE (co-cultures). RGD and RGDp increased nanoparticle transport by M cells. The specific targeting of the β1 integrins by the RGD- and RGDp-nanoparticles was dem-

onstrated by the inhibition of their transport by anti-β1 integrin. Mannose was also able to increase the transport of nanoparticles by M cells compared to that of non-targeted nanoparticules. However, this ligand was not specific to M cells since the transport of man-nanoparticles was also improved by enterocytes. These results could be explained by the presence of a mannose receptor at the apical surface of human enterocytes. Although this receptor has been reported to be overexpressed in mouse FAE [35,36], we could not confirm its presence in our *in vitro* model (unpublished results). Mannose presence at the nanoparticle surface could modify their bioadhesion to the intestinal mucosa, promoting their uptake by enterocytes (mono-cultures), APC or DC inserted in the epithelium and M cells (co-cultures) [37,38]. This adhesive mechanism could be related to the high binding affinity of mannose residues to the mannose-binding lectins that are expressed on the lymphoid and non-lymphoid cells of the gut [39,40].

M cells are now considered as a major protagonist in the development of oral vaccine formulations, many efforts being focused on the improvement of the transcytosis of antigen-loaded nanoparticles by M cells. However, it is well known that APC such as DCs and macrophages also play an important role in the induction of the immune response after oral immunization. Mouse and human DCs and macrophages have been shown to express a mannose receptor, and this receptor has been exploited to deliver antigens, resulting in a more robust immune response [21–23,41]. Uptake studies by macrophages were carried out to investigate whether the labeling of nanoparticles with the different ligands can enhance the *in vitro* uptake of the nanoparticles by a mouse macrophage cell line. As expected [21], the uptake of mannose-labeled nanoparticles by macrophages was enhanced. The presence of ligand such as RGD, LDVd, and LDVp at the nanoparticle surface also increased their uptake by macrophages compared to non-targeted nanoparticles.

Both intragastric and intraduodenal immunizations with ovalbumin-loaded nanoparticles effectively induced an immune response. However, this immune response and the number of responding mice were significantly increased after intraduodenal administration, when compared to the delivery by gavage. Specific anti-ovalbumin IgG was detected in the sera of some of the mice immunized by gavage, while all mice immunized by intramuscular produced specific IgG antibodies. The presence of non-responders in orally vaccinated mice has been frequently reported in different studies [42–44]. Moreover, some immunization studies used high oral doses of encapsulated antigen and successive administrations to obtain significant immune responses in mice, even with potent immunogens such as BSA or ovalbumin [45,46]. Intragastric administration of LDVd-nanoparticles elicited in three out of eight mice a higher IgG titer than after IM injection of free ovalbumin. Moreover, LDVd- nanoparticles induced significant levels of IgG2a antibodies after intragastric administration compared to the absence of this isotype elicited by the IM injection and by the free oral peptide (data not shown).

When nanoparticles were administered by the intraduodenal route, the immune response was significantly increased. The higher response induced by intraduodenal injection could be due to a higher concentration of local nanoparticles in the duodenum and/or no degradation by the harsh gastric environment and enzymes. The different ligands present at the nanoparticle surface increased the IgG response compared with non-targeted nanoparticles. RGDp, LDVd and mannose labeling of nanoparticles elicited a stronger immune response after intraduodenal administration with a higher production of IgG than after IM injection of non-adjuvanted ovalbumin. Although all groups except mice immunized with free ovalbumin elicited a mixed IgG1/IgG2a response, the IgG1 subclasses were predominantly expressed. However, the immune response was more balanced for the groups immunized with the nanoparticles when compared to mice immu-

nized by IM. This is consistent with other reports stating that the major difference between the immune response elicited by conventional formulation and PLGA particles is the induction of a balanced Th1 and Th2 responses to PLGA particles compared to Th2 response to free OVA [47]. All the formulations were able to induce a cellular immune response, as shown by the IFN-γ production in splenocytes. However, some differences were observed in this IFN-γ production in function of the ligand grafted at the nanoparticle surface, suggesting a different process in the induction of the immune response, possibly due to a different recognition by the APC.

The high immunization obtained after immunization with RGDp, LDVd and man-nanoparticles could be explained in part by the improved transport of those formulations by the M-like cells and/or by their better internalization by macrophages compared to other formulations. On the basis of results obtained in the present study, it is very difficult to determine whether the best strategy is to target the apical surface of M cells or to target the immune cells present in their basolateral pocket. Indeed, RGDp-nanoparticles showed increased transport in the *in vitro* model, but were poorly internalized by macrophages. On the contrary, LDVd-nanoparticles were very weakly transported *in vitro* but their uptake by macrophage was high. Mannose-grafted nanoparticles were transported by enterocytes and M cells and internalized well by macrophages. *In vivo*, we demonstrated that the use of all of these ligands at the nanoparticle surface allowed an increase in the specific IgG production in the sera of mice after intraduodenal immunization, confirming the importance of targeting the carriers towards M cells or immune cells. The cellular immune response seen after intraduodenal administration indicates that a different immune response occurs with different ligands present on the surface of the nanoparticle. This could be attributed to the variations of uptake of these particles by M cells and/or APC, thus causing a change in the induction pathway. The comparison with data reported by other groups is difficult because antigen, dose, timing of priming and boost(s) as well as IgG titer definition widely differ. However, the presence of ligands such as vitamin B12 [48] or thiamine [34] has been shown to enhance immune response after oral delivery.

The increased transmucosal uptake of vaccine particles via the targeting of M cells or of immune cells influenced the profile and the intensity of the immune response obtained after intraduodenal vaccination. Optimal oral vaccination effects with nanoparticle delivery systems should therefore be achieved with formulations having both M cell targeting molecules in addition to ligands of the APCs of the lymphoid tissue. The addition of a mucosal adjuvant in the formulation could also be considered.

References

[1] N. Foster, B.H. Hirst, Exploiting receptor biology for oral vaccination with biodegradable particulates, Adv. Drug Deliv. Rev. 57 (3) (2005) 431–450.

[2] S.A. Galindo-Rodriguez, E. Allemann, H. Fessi, E. Doelker, Polymeric nanoparticles for oral delivery of drugs and vaccines: a critical evaluation of in vivo studies, Crit. Rev. Ther. Drug Carrier Syst. 22 (5) (2005) 419–464.

[3] J. Holmgren, C. Czerkinsky, Mucosal immunity and vaccines, Nat. Med. 11 (Suppl. 4) (2005) S45–S53.

[4] E.C. Lavelle, D.T. O'Hagan, Delivery systems and adjuvants for oral vaccines, Expert. Opin. Drug Deliv. 3 (6) (2006) 747–762.

[5] D.S. Silin, O.V. Lyubomska, V. Jirathitikal, A.S. Bourinbaiar, Oral vaccination: where we are?, Expert Opin. Drug Deliv. 4 (4) (2007) 323–340.

[6] L.J. Peek, C.R. Middaugh, C. Berkland, Nanotechnology in vaccine delivery, Adv. Drug Deliv. Rev. 60 (8) (2008) 915–928.

[7] V.H.L. Lee, A. Yamamoto, Penetration and enzymatic barriers to peptide and protein absorption, Adv. Drug Deliv. Rev. 4 (2) (1989) 171–207.

[8] A. des Rieux, V. Fievez, M. Garinot, Y.J. Schneider, V. Preat, Nanoparticles as potential oral delivery systems of proteins and vaccines: a mechanistic approach, J. Control. Release 116 (1) (2006) 1–27.

[9] A. Gebert, H.J. Rothkotter, R. Pabst, M cells in Peyer's patches of the intestine, Int. Rev. Cytol. 167 (1996) 91–159.

[10] A. Gebert, I. Steinmetz, S. Fassbender, K.H. Wendlandt, Antigen transport into Peyer's patches: increased uptake by constant numbers of M cells, Am. J. Pathol. 164 (1) (2004) 65–72.

[11] M.R. Neutra, P.J. Sansonetti, J.P. Kraehenbuhl, M Cells and Microbial Pathogens, Raven Press, Berlin, 2003. pp. 163–178.

[12] M. Garinot, V. Fievez, V. Pourcelle, F. Stoffelbach, A. des Rieux, L. Plapied, I. Theate, H. Freichels, C. Jerome, J. Marchand-Brynaert, Y.J. Schneider, V. Preat, PEGylated PLGA-based nanoparticles targeting M cells for oral vaccination, J. Control. Release 120 (3) (2007) 195–204.

[13] E. Gullberg, M. Leonard, J. Karlsson, A.M. Hopkins, D. Brayden, A.W. Baird, P. Artursson, Expression of specific markers and particle transport in a new human intestinal M-cell model, Biochem. Biophys. Res. Commun. 279 (3) (2000) 808–813.

[14] U. Hersel, C. Dahmen, H. Kessler, RGD modified polymers: biomaterials for stimulated cell adhesion and beyond, Biomaterials 24 (24) (2003) 4385–4415.

[15] S. Biltresse, M. Attolini, G. Dive, A. Cordi, G.C. Tucker, J. Marchand-Brynaert, Novel RGD-like molecules based on the tyrosine template: design, synthesis, and biological evaluation on isolated integrins alphaVbeta3/alphaIIbbeta3 and in cellular adhesion tests, Bioorg. Med. Chem. 12 (20) (2004) 5379–5393.

[16] S. Biltresse, M. Attolini, J. Marchand-Brynaert, Cell adhesive PET membranes by surface grafting of RGD peptidomimetics, Biomaterials 26 (22) (2005) 4576–4587.

[17] D. Heckmann, A. Meyer, B. Laufer, G. Zahn, R. Stragies, H. Kessler, Rational design of highly active and selective ligands for the alpha5beta1 integrin receptor, Chembiochem. 9 (9) (2008) 1397–1407.

[18] S.P. Adams, R.R. Lobb, Inhibitors of integrin alpha ' beta 1 (VLA-4), Ann. Rep. Med. Chem. 34 (179–188) (1999).

[19] K. Lin, H.S. Ateeq, S.H. Hsiung, L.T. Chong, C.N. Zimmerman, A. Castro, W.C. Lee, C.E. Hammond, S. Kalkunte, L.L. Chen, R.B. Pepinsky, D.R. Leone, A.G. Sprague, W.M. Abraham, A. Gill, R.R. Lobb, S.P. Adams, Selective, tight-binding inhibitors of integrin alpha4beta1 that inhibit allergic airway responses, J. Med. Chem. 42 (5) (1999) 920–934.

[20] M. Momtaz, V. Rerat, S. Gharbi, E. Gerard, V. Pourcelle, J. Marchand-Brynaert, A graftable LDV peptidomimetic: design, synthesis and application to a blood filtration membrane, Bioorg. Med. Chem. Lett. 18 (3) (2008) 1084–1090.

[21] V. Apostolopoulos, N. Barnes, G.A. Pietersz, I.F. McKenzie, Ex vivo targeting of the macrophage mannose receptor generates anti-tumor CTL responses, Vaccine 18 (27) (2000) 3174–3184.

[22] A.J. Engering, M. Cella, D. Fluitsma, M. Brockhaus, E.C. Hoefsmit, A. Lanzavecchia, J. Pieters, The mannose receptor functions as a high capacity and broad specificity antigen receptor in human dendritic cells, Eur. J. Immunol. 27 (9) (1997) 2417–2425.

[23] A.J. Engering, M. Cella, D.M. Fluitsma, E.C. Hoefsmit, A. Lanzavecchia, J. Pieters, Mannose receptor mediated antigen uptake and presentation in human dendritic cells, Adv. Exp. Med. Biol. 417 (1997) 183–187.

[24] H.R. Kricheldorf, J.M. Jonte, M. Berl, Polylactones. 3. Copolymerization of glycolide with ʟʟ-lactide and other lactones, Makromol. Chem. 12 (1985) 25–38.

[25] L.W. Cao, H. Wang, J.S. Li, H.S. Zhang, 6-Oxy-(N-succinimidyl acetate)-9-(2'-methoxycarbonyl)fluorescein as a new fluorescent labeling reagent for aliphatic amines in environmental and food samples using high-performance liquid chromatography, J. Chromatogr. A 1063 (1–2) (2005) 143–151.

[26] M.L. Zweers, G.H. Engbers, D.W. Grijpma, J. Feijen, In vitro degradation of nanoparticles prepared from polymers based on ᴅʟ-lactide, glycolide and poly(ethylene oxide), J. Control. Release 100 (3) (2004) 347–356.

[27] C.A. Nguyen, E. Allemann, G. Schwach, E. Doelker, R. Gurny, Cell interaction studies of PLA-MePEG nanoparticles, Int. J. Pharm. 254 (1) (2003) 69–72.

[28] P. Vangeyte, R. Jerome, Amphiphilic block copolymers of high-molecular-weight poly(ethylene oxyde) and either epsilon-caprolactone or gamma-methyl-epsilon caprolactone: synthesis and characterization, J. Pharmacol. Exp. Ther. 42 (1132–1142) (2004).

[29] V. Pourcelle, H. Freichels, F. Stoffelbach, R. uzely-Velty, C. Jerome, J. Marchand-Brynaert, Light induced functionalization of PCL–PEG block copolymers for the covalent immobilization of biomolecules, Biomacromolecules (2009), doi:10.1021/bm900027r.

[30] V. Pourcelle, S. Devouge, M. Garinot, V. Preat, J. Marchand-Brynaert, PCL–PEG-based nanoparticles grafted with GRGDS peptide: preparation and surface analysis by XPS, Biomacromolecules 8 (2007) 3977–3983.

[31] D. Lemoine, M. Deschuyteneer, F. Hogge, V. Preat, Intranasal immunization against influenza virus using polymeric particles, J. Biomater. Sci. Polym. Ed. 10 (8) (1999) 805–825.

[32] A. des Rieux, V. Fievez, I. Theate, J. Mast, V. Preat, Y.J. Schneider, An improved in vitro model of human intestinal follicle-associated epithelium to study nanoparticle transport by M cells, Eur. J. Pharm. Sci. 30 (5) (2007) 380–391.

[33] P. Artursson, Epithelial transport of drugs in cell culture. I: a model for studying the passive diffusion of drugs over intestinal absorptive (Caco-2) cells, J. Pharm. Sci. 79 (6) (1990) 476–482.

[34] H.H. Salman, C. Gamazo, M. Agueros, J.M. Irache, Bioadhesive capacity and immunoadjuvant properties of thiamine-coated nanoparticles, Vaccine 25 (48) (2007) 8123–8132.

[35] K. Hase, S. Ohshima, K. Kawano, N. Hashimoto, K. Matsumoto, H. Saito, H. Ohno, Distinct gene expression profiles characterize cellular phenotypes of follicle-associated epithelium and M cells, DNA Res. 12 (2) (2005) 127–137.

[36] D. Lo, W. Tynan, J. Dickerson, J. Mendy, H.W. Chang, M. Scharf, D. Byrne, D. Brayden, L. Higgins, C. Evans, D.J. O'Mahony, Peptidoglycan recognition protein expression in mouse Peyer's Patch follicle associated epithelium suggests functional specialization, Cell Immunol. 224 (1) (2003) 8–16.

[37] H.H. Salman, C. Gamazo, M.A. Campanero, J.M. Irache, Salmonella-like bioadhesive nanoparticles, J. Control. Release 106 (1–2) (2005) 1–13.

[38] H.H. Salman, C. Gamazo, M.A. Campanero, J.M. Irache, Bioadhesive mannosylated nanoparticles for oral drug delivery, J. Nanosci. Nanotechnol. 6 (9–10) (2006) 3203–3209.

[39] F. Dalle, T. Jouault, P.A. Trinel, J. Esnault, J.M. Mallet, P. d'Athis, D. Poulain, A. Bonnin, Beta-1,2- and alpha-1,2-linked oligomannosides mediate adherence of Candida albicans blastospores to human enterocytes in vitro, Infect. Immun. 71 (12) (2003) 7061–7068.

[40] S. Wagner, N.J. Lynch, W. Walter, W.J. Schwaeble, M. Loos, Differential expression of the murine mannose-binding lectins A and C in lymphoid and nonlymphoid organs and tissues, J. Immunol. 170 (3) (2003) 1462–1465.

[41] R. Jordens, A. Thompson, R. Amons, F. Koning, Human dendritic cells shed a functional, soluble form of the mannose receptor, Int. Immunol. 11 (11) (1999) 1775–1780.

[42] O. Borges, J. Tavares, S.A. de, G. Borchard, H.E. Junginger, A. Cordeiro-da-Silva, Evaluation of the immune response following a short oral vaccination schedule with hepatitis B antigen encapsulated into alginate-coated chitosan nanoparticles, Eur. J. Pharm. Sci. 32 (4–5) (2007) 278–290.

[43] M.J. McCluskie, R.D. Weeratna, H.L. Davis, Intranasal immunization of mice with CpG DNA induces strong systemic and mucosal responses that are influenced by other mucosal adjuvants and antigen distribution, Mol. Med. 6 (10) (2000) 867–877.

[44] M.J. McCluskie, R.D. Weeratna, A.M. Krieg, H.L. Davis, CpG DNA is an effective oral adjuvant to protein antigens in mice, Vaccine 19 (7–8) (2000) 950–957.

[45] I. Gutierro, R.M. Hernandez, M. Igartua, A.R. Gascon, J.L. Pedraz, Influence of dose and immunization route on the serum IgG antibody response to BSA loaded PLGA microspheres, Vaccine 20 (17–18) (2002) 2181–2190.

[46] I. Gutierro, R.M. Hernandez, M. Igartua, A.R. Gascon, J.L. Pedraz, Size dependent immune response after subcutaneous, oral and intranasal administration of BSA loaded nanospheres, Vaccine 21 (1–2) (2002) 67–77.

[47] T. Storni, T.M. Kundig, G. Senti, P. Johansen, Immunity in response to particulate antigen-delivery systems, Adv. Drug Deliv. Rev. 57 (3) (2005) 333–355.

[48] H.H. Salman, C. Gamazo, P.C. de Smidt, G. Russell-Jones, J.M. Irache, Evaluation of bioadhesive capacity and immunoadjuvant properties of vitamin B(12)–Gantrez Nanoparticles, Pharm. Res. 25 (12) (2008) 2859–2868.